ICANS-XV
15th Meeting of the International Collaboration on Advanced
Neutron Sources
November 6-9, 2000
Tsukuba, Japan

23.15
Water Flow Experiment using the PIV Technique and the Thermal Hydraulic Analysis on the Cross-Flow Type Mercury Target Model

Katsuhiro Haga*, Atsuhiko Terada, Masanori Kaminaga and Ryutaro Hino

Japan Atomic Energy Research Institute (JAERI)
2-4 Shirakata-Shirane, Tokai-mura, Naka-gun, Ibaraki-ken, 319-1195, Japan
*E-mail : haga@cat.tokai.jaeri.go.jp

Abstract

In this study the effectiveness of the cross-flow type mercury target structure was evaluated experimentally and analytically. The average water flow velocity field in the target mock-up model, which was fabricated with plexiglass, was measured at room temperature using the PIV technique. The water flow analyses were conducted and the analytical results were compared with the experimental results. The experimental results showed that the cross-flow could be realized in the former part of the proton beam path where the heat load by the spallation reaction is large, and the analytical result of the water flow velocity field showed good correspondence to the experimental result in the case of the Reynolds number of more than 4.83×10^5 at the model inlet. With these results, the effectiveness of the cross-flow type mercury target structure and the present analysis code system was demonstrated. Then the mercury flow field and the temperature distribution in the target container were analyzed assuming the proton beam energy and power of 3GeV and 5MW. The analytical result showed that the cross-flow field of mercury, which is similar to the water flow field, could also be attained.

1. Introduction

In the proton beam path of the target, vast amount of heat is generated by the spallation reaction. If a stagnant region is generated in the proton beam path by the recirculation flow, excessive temperature rise and boiling of the mercury will arise there, which will cause degradation of the neutronic performance and the structural integrity, and flow-induced vibration. Thus suppressing the creation of the recirculation region in the proton beam path is very important for the mercury target container design.

In order to meet this technical demand, JAERI proposed the cross-flow type target container in which the mercury flows across the proton beam path, and has continued the optimization of the flow channel structure with the thermal-hydraulic analysis code. Through the analytical works, we got the prospect to achieve the cross-flow velocity distribution that conforms to the heat load distribution along the proton beam path by using the flow guide plates [1]. Based on these results, we fabricated a plexiglass mock-up model of the cross-flow type target in order to verify the analytical results under water flow conditions.

In this study, the experimental result of the water flow velocity field in the mock-up target model measured with the Particle Image Velocimetry (PIV) technique [2] and the analytical result conducted with the standard k-ε turbulent model are reported to evaluate the validity of the analysis code and the cross-flow type target geometry. The analytical results of the mercury flow and the temperature field, assuming the proton beam energy and power of 3GeV and 5MW, are also reported.

2. Experimental set-up

Fig. 1 shows the water loop used in this experiment. Water is supplied to the target model from the reservoir tank, of which capacity is $3m^3$, by a water pump. The rated flow rate of the water pump is $5m^3/min$. A heat exchanger is installed at the outlet of the target model to prevent the water temperature rise by the pump heat injection. The water flow rate is measured with an electro-magnetic flow meter and is regulated by the rotational frequency of the

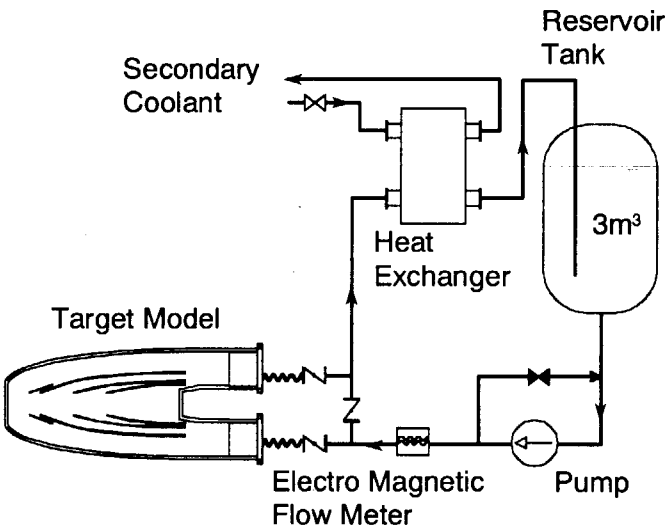

Fig. 1 Water loop for the target experiment

water pump.

Fig. 2 shows a picture of the PIV system devices. Very fine particles are mixed in the water as light reflectors and they flow in the target model. They are irradiated by pulse laser sheets with very short intervals of ca. 50μs. Pictures of the flow field in the target model are taken with a CCD camera with the same timing as the laser sheet emission. Two adjacent pictures are compared digitally and the water flow velocities are calculated with the moved distances of the particles seen on the CCD camera images.

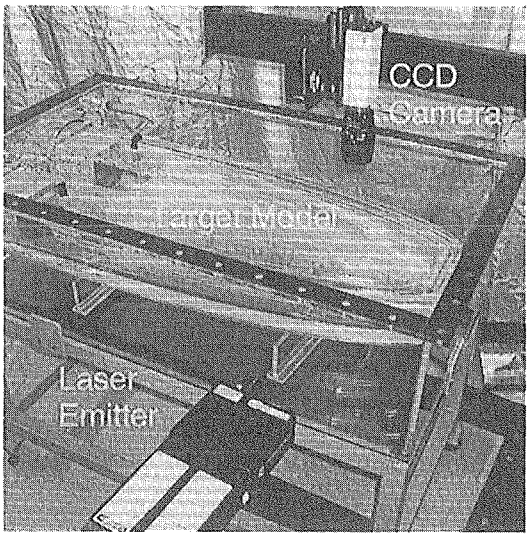

Fig. 2 Experimental setup of the PIV system

Fig. 3 shows the structure and the dimensions of the mock-up model of the mercury target used for the water experiment. This model was designed assuming proton beam power of 5MW, proton energy of 1.5GeV, and rectangular cross section of proton beam of 68.8mm x 100mm. The model was made of transparent plexiglass for the flow velocity field measurement by the PIV technique. The inner structure and the dimensions of the model are the same as that of the mercury target. Four flow guide plates of 5mm thickness are placed on both sides of the proton beam path which is 100mm in width and is shown as the hatched area in the figure. The water flow crosses the proton beam path area between the flow guide plates. In the following discussions, we distinguish the flow channels between the flow guide plates with numbers as shown in Fig. 3 and express the position in the target model with the position on the x axis of which origin is set on the inner surface of the beam window. Since the heat generation density by the spallation reaction reaches its peak near the beam window, which is 1.9kW/cm^3 in the 5MW target system with the proton beam energy of 3GeV, plenty of mercury

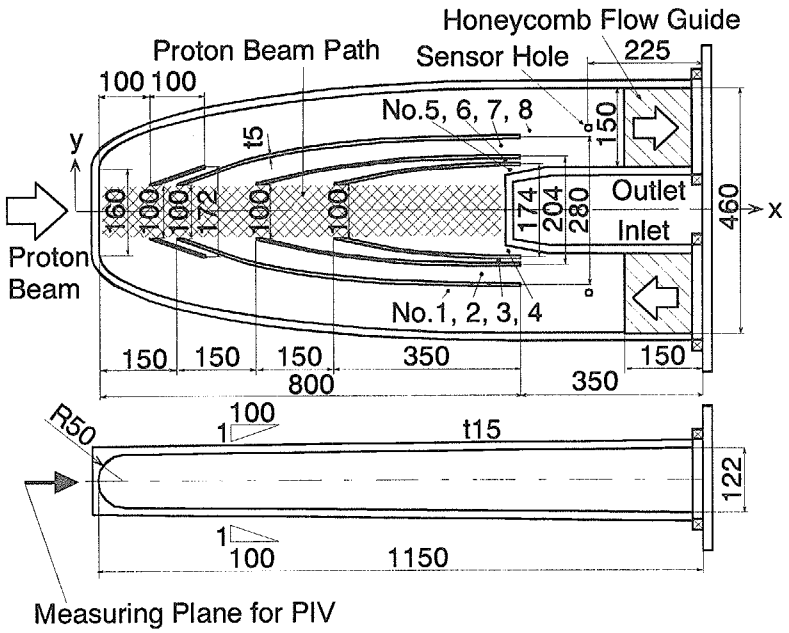

Fig. 3 Experimental model of the cross-flow type mercury target

should be distributed to No. 1 channel along which the mercury flow is guided to the beam window. In order to increase the flow rate in No. 1 channel, the flow channel gaps were decreased, to increase the flow resistance, as their position approaches the center axis of the model. The model was submerged in a water bath to minimize the deformation of the laser sheet on the rounded surface of the model.

3. Experimental condition

While the water temperature is room temperature (300K) at the model inlet, the mercury temperature is designed to be 323K (50 deg C) at the inlet of the mercury target. By comparing the kinematic viscosities of water and mercury under these conditions, it is known that the water flow velocity approximately 8.2 times higher than the mercury flow velocity is needed to equalize the Reynolds number at the target inlet and to simulate the mercury flow with the water flow. This Reynolds number is introduced as the tentative standard in comparison with the water and the mercury flow in the target container. The maximum water velocity at the model inlet was set to 5m/s in order to secure the solidity of the plexiglass model against the inner pressure. This water velocity corresponds to the Reynolds number of 8.05×10^5 and to the mercury flow velocity of 0.6m/s. The measuring plane was set at the center level of the model height horizontally, as is shown in Fig. 3.

4. Analytical method and model

In order to compare the experimental results of the water flow with the analytical results and to simulate the mercury flow field, we conducted the computational analysis using the three dimensional model of the same structure with the experimental model. The conventional thermal hydraulic analysis code, STAR-CD, was used. The analytical methods are as follows:

Analytical scheme	: Finite volume method
Solution Algorithm	: SIMPLE method
Spatial discretisation scheme	: Quadratic upstream interpolation of convective kinematics (QUICK)
Turbulence model	: Standard k-ε model
Wall boundary condition	: Law of the wall

The analytical model is a half model assuming mirror symmetry with respect to the horizontal plane at the midpoint of the target model. The cell shape is hexahedral and the total cell number is 242632.

5. Water flow experiment and analysis

5.1 Experimental results

Fig. 4 shows the vector map of the water velocity under the condition of inlet flow velocity of 5m/s. The flow velocity at the No. 1 channel inlet is about 3.8m/s, which is slightly slower than the average velocity at the model inlet, but the flow velocity at the other channel inlets are faster than the model inlet velocity. The flow velocity is about 7m/s at the No. 2 channel inlet, and 10m/s at the No. 3 and the No. 4 channel inlets. The mass flow percentages are ca. 40% in No. 1 channel, ca. 32% in No. 2 channel, ca. 14% in No. 3 and No. 4 channels. These percentages were calculated with the inlet velocities of each channel multiplied by the channel cross sections. As we intended, more than 40% of the whole inlet water was distributed to No. 1 channel and that increased the flow velocity near the beam window where the heat generation density is the largest. The cross-flow field was successfully realized from x=0mm to x=450mm where the volumetric heat generation rate is high. Although there is a large recirculation flow in the area from x=450mm to x=750mm, the temperature rise in the area appeared to be modest in the mercury flow analysis which will be mentioned later. Part of the water flow of No. 2 channel joined with the water flow of No. 1 channel, which made the flow velocity large at the inlet of No. 8 channel. The separation flows and small vortices were generated in the downstream side of the flow guide plates at the inlet of No. 7 and No. 8 channels. Because these vortices are out of the proton beam path,

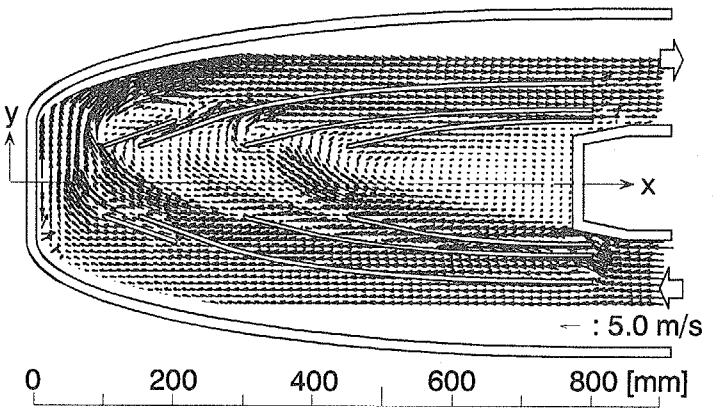

Fig. 4 Experimental result of the water flow Field (Inlet velocity : 5m/s)

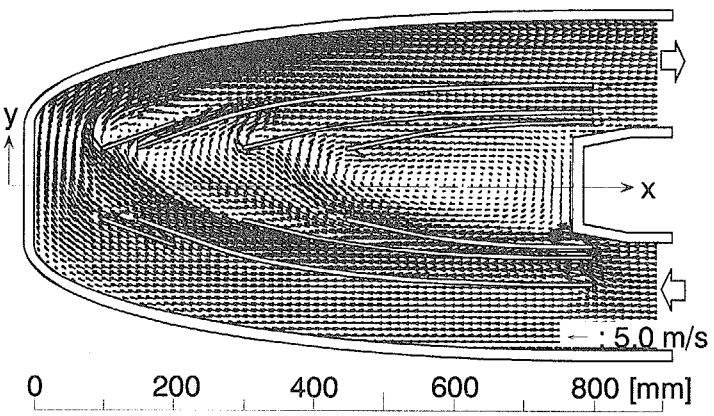

Fig. 5 Analytical result of the water flow Field (Inlet velocity : 5m/s)

they are not considered to be the cause of the excessive temperature rise of mercury.

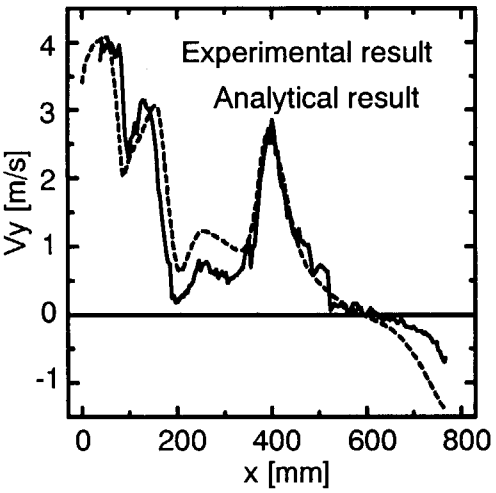

Fig. 6 Experimental and analytical result of the Vy distribution along the center axis (Inlet velocity : 5m/s)

5.2 Analytical result

For the water flow analysis, the water temperature was set to room temperature and the water flow velocity at the inlet of the model was set to 5m/s. The volumetric heat generation was not considered.

By comparing the analytical result of the flow pattern in Fig. 5 with the experimental result in Fig. 4, it can be seen that the flow pattern of the whole flow velocity field of the analytical result corresponds well to the experimental result. Several characteristic flow patterns seen in the experimental results are simulated successfully. For example, the large flow velocity at the inlet of No. 3 and No. 4 channels, also the large flow velocity at the front end of the flow guide plate of No. 8 channel, the shape of the jet flow crossing the proton beam path, and the separation flows at the downstream side of the flow guide plates. The recirculation flow seen in the area over x=450mm is also simulated well.

Fig. 6 shows the experimental and the analytical results of the y-component (Vy) distribution of the flow velocity along the center axis (x). The Vy distribution patterns also show the good correspondence. The Vy value is especially well simulated quantitatively near the proton beam window where sufficient flow rate is necessary for the swift cooling of the spallation heat. But the analytical result is about 100% larger than the experimental result from x=200mm to x=350mm, where the jet flow from No.3 channel crosses the proton beam path. The reason of this difference is thought to be the pressure loss increase in No. 3 channel due to the deformation of the flow guide plates caused by the pressure difference between the flow channels. In the rear part of the proton beam path, the Vy peak by the jet flow from No. 4 channel at x=400mm and the center of the recirculation flow at x=600mm are also simulated quantitatively well.

With these results, the present analysis code is considered to be effective to analyze the fluid flow field of high Reynolds number in the target container.

6. Mercury flow analysis

As mentioned before, mercury will be used as the target material for the actual neutron scattering facility, so the flow structure of the mercury in the target container is what we are most interested in. Using the present analysis code and the computational model, of which effectiveness was demonstrated in the former section, we conducted thermal and hydraulic analysis assuming mercury as the coolant fluid.

6.1 Analytical condition

For the mercury flow analysis, the inlet mercury temperature was set to 50 deg C and the inlet velocity was set to 0.6m/s, 1.0m/s, 1.5m/s and 2m/s. The volumetric heat generation was considered. Although the experimental model was originally designed assuming the proton energy of 1.5GeV, it has changed to 3GeV in the present accelerator design. So, the mercury flow analyses was conducted assuming the proton energy and power of 3GeV and 5MW. The distribution of the volumetric heat generation rate (Q) in the mercury target used in the analysis is shown in Fig. 7. This was computed by the neutronic code system NMTC/JAERI and is expressed by the following correlation.

$$Q = 4233.5*(1.-2.1682*EXP(-0.17587*(x+10.148)))*EXP(-0.061024*(x+12.14))) \quad [MW/m^3]$$

In the mercury flow analysis, the Q value was multiplied by 1.4 to include safety margin. Fig. 7 shows the multiplied value. The thermal condition at the wall boundary was set to adiabatic except the proton beam window wall where the heat income from the wall was set to 255W/cm^2. The turbulent Prandtl number was set to 1.5. The physical properties of mercury were assumed to be constant and they were set at the temperature of 50 deg C under the pressure of 0.1MPa as follows:

Density : 13472.51 kg/m^3
Viscosity : 1.41 x 10^{-3} kg/m/K
Specific heat capacity : 138.5 J/kg/K
Thermal conductivity : 9.36 W/m/K

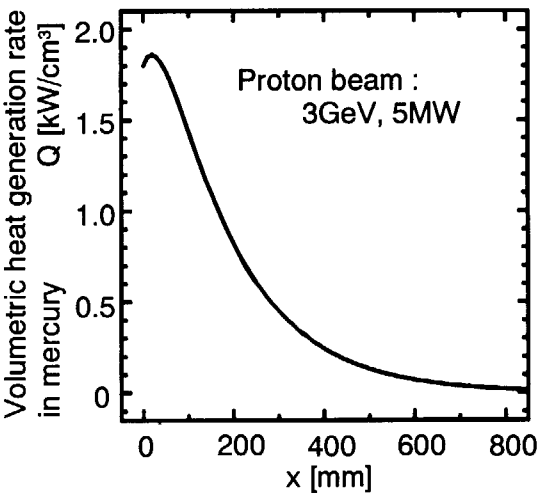

Fig. 7 Distribution of the volumetric heat generation rate including 40% margin

6.2 Analytical results

Since the analytical results of the flow patterns and the temperature distributions were similar in all cases, the flow velocity and the temperature contour maps in the case of the inlet velocity of 1.5m/s are shown in Fig. 8 and Fig. 9 as the representative case.

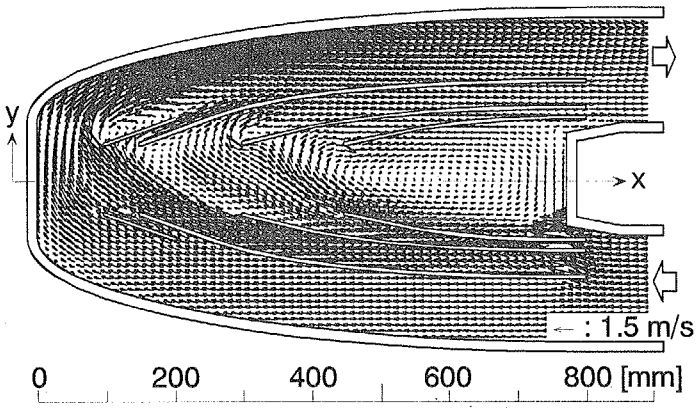

Fig. 8 Analytical result of the mercury flow field (Inlet velocity : 1.5m/s)

The flow field pattern of mercury shown in Fig. 8 is almost the same as the water flow field shown in Fig. 5. The larger flow velocity near the proton beam window and the cross flow in the proton beam path were also realized in the mercury flow. The maximum velocity is 3.7m/s at the inlet of the number 3 channel.

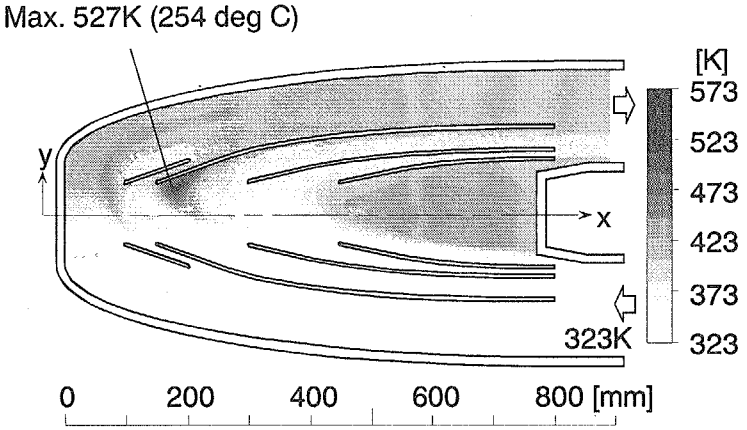

Fig. 9 Analytical result of the mercury temperature field (Inlet velocity : 1.5m/s)

Fig. 9 shows that the mercury temperature is under 473K (200 deg C) in most of the flow field. The maximum temperature is 527K (254 deg C) at the inner side of the flow guide plate where the mercury flow from No. 3 channel impinges and the flow velocity slows. Looking at the recirculation area in the rear of the proton beam path, the temperature rise is modest, 439K (166 deg C), at the center of the recirculation, because the heat generation density in the area is relatively low as shown in Fig. 7, which is under 100W/cm^3 in the 5MW target system. So this recirculation is not considered to cause the excessive temperature rise.

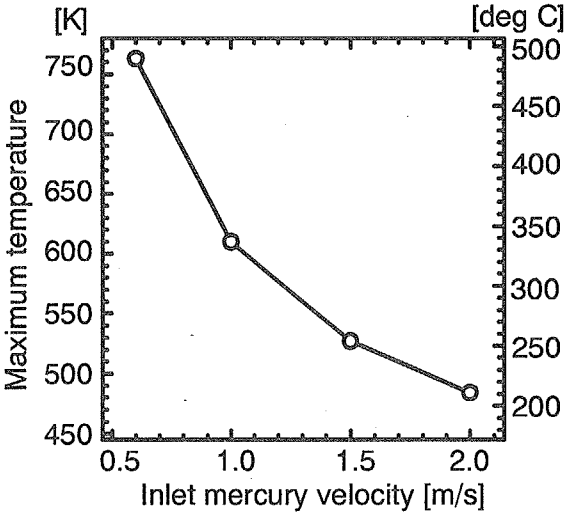

Fig. 10 Maximum temperature dependence on the inlet mercury velocity

Fig. 10 shows the maximum mercury temperature dependence on the inlet mercury velocity. As the mercury velocity becomes higher, the spallation heat cooling would be easier at the sacrifice of the target container lifetime which will be shortened by target wall erosion. The design criteria for maximum mercury velocity in the target container will be determined with the trade-off between those two factors. The lifetime of the target container is set to at least 6 months from the viewpoint of the irradiation damage. Considering the target wall thickness of 3mm in the present design, the mercury velocity should be as low as possible. The heat conduction through the flow guide plate, which was not taken into account in this analysis, would contribute to the decline of the maximum temperature and it will lead to the lower mercury velocity in the target. Correlation between the mercury velocity and the erosion speed needs to be investigated in the material researches.

7. Transient flow (Experimental results)

As shown in Fig. 9, the hot spot was generated at the inner side of the flow guide plate where the mercury flow velocity slowed. Because the analysis was conducted under the steady state condition, the temperature field of Fig. 9 is based on the fixed flow field shown in Fig. 8. Considering that the flow field in the target container is essentially transient, it is expected that the transient effect might promote the turbulent heat transfer in the mercury and make the maximum temperature lower. In order to observe the transient flow field at the hot spot position, we made the animation with the vector map images of the water flow measured by the PIV system. 100 images taken at intervals of one second were used for the animation.

Fig. 11 shows the sequence of the flow field vector map images at intervals of two seconds. The velocity vectors near the flow guide plate on the right side are not shown because the flow field could not be measured due to the reflection of the laser sheet at the surface of the flow guide plate. Although the average flow velocity is low at the hot spot position, the flow direction and the velocity magnitude of the instantaneous flow vectors vary greatly. It can be seen in the figure that the flow velocity at the hot spot is almost zero at 0s, but the stagnant area is swept by the small vortices and disappears with several second intervals. The influence of the transient flow on the maximum temperature of mercury will be analyzed in future work.

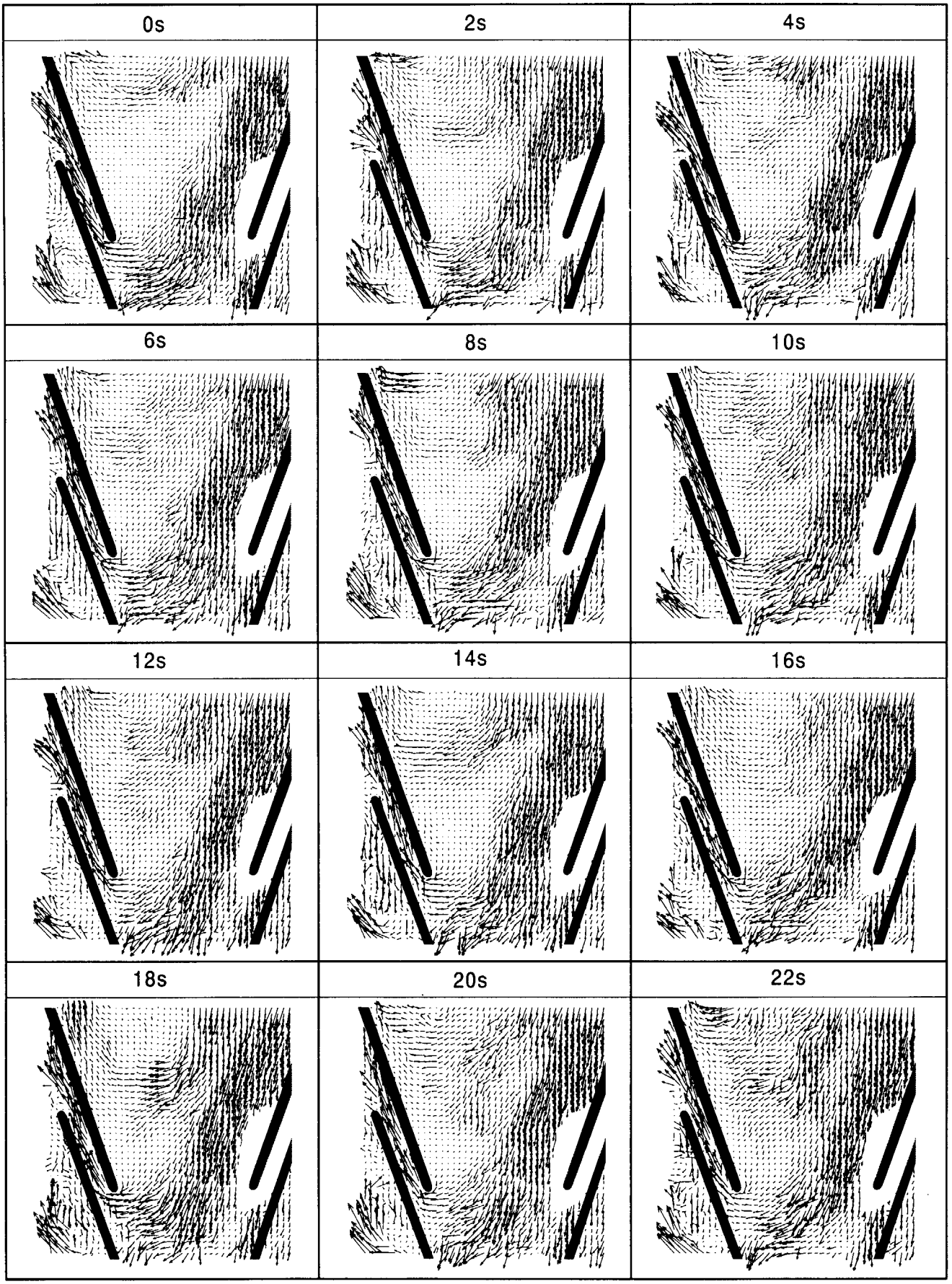

Fig. 11 Sequence of the instantaneous water flow fields at the hot spot position measured by PIV

8. Concluding remarks

The average water flow behavior in the mock-up model of the cross-flow type mercury target was studied experimentally at room temperature using the PIV technique. The water flow analyses were also conducted with the general computational fluid dynamics code, STAR-CD, and the experimental results were compared with the analytical results to evaluate the effectiveness of the present computational model and the code system. Then, the mercury flow field and the temperature distribution in the target container were analyzed assuming the proton beam energy and power of 3GeV and 5MW. The obtained results are summarized as follows:

(1) It was confirmed in the water experiment that the cross flow, which is the characteristic of the cross flow type target, could be realized in most of the proton beam path area where the removal of the high density heat is important.

(2) Using the standard k-ε model and the high-order discretisation scheme (QUICK), the water flow field in the target container was analyzed and the analytical result showed good correspondence to the experimental result. With this, the effectiveness of the present analysis code to simulate the liquid flow field in the target container was demonstrated.

(3) Using the same computational model and the analytical scheme as those for water flow analysis, the mercury flow field in the target container was analyzed. The analytical result showed that the cross-flow field of mercury could be attained in the former part of the proton beam path where the heat load by the spallation reaction is large.

(4) The recirculation flow seen in the rear of the proton beam path is considered to cause no excessive temperature rise.

References

[1] M. Kaminaga, A. Terada, S. Ishikura, M. Teshigawara, Y. Sudo, R. Hino, Mercury target development for JAERI spallation neutron source., Proc. 7th international conference on nuclear engineering(ICONE-7), Tokyo, ICONE-7123, (1999).

[2] M. Raffel, C.E. Willert, J. Kompenhans, Particle Image Velocimetry, Springer Verlag Published (1998)